

Standoff Detection of Explosives at 1 m using Laser Induced Breakdown Spectroscopy

Rajendhar Junjuri[#], Ashwin Kumar Myakalwar^{#,*}, and Manoj Kumar Gundawar^{#,*}[#]Advanced Centre of Research in High Energy Materials, University of Hyderabad, Hyderabad - 500 046, India[@]Institute of Photonics and Electronics, Czech Academy of Sciences, Prague -182 51, Czech Republic^{*}E-mail: manoj@uohyd.ac.in

ABSTRACT

We report the 'standoff detection' of explosives at 1 m in laboratory conditions, for the first time in India, using Laser Induced Breakdown Spectroscopy combined with multivariate analysis. The spectra of a set of five secondary explosives were recorded at a distance of 1 m from the focusing as well as collection optics. The plasma characteristics viz., plasma temperature and electron density were estimated from Boltzmann statistics and Stark broadening respectively. Plasma temperature was estimated to be of the order of $(10.9 \pm 2.1) \times 10^3$ K and electron density of $(3.9 \pm 0.5) \times 10^{16}$ cm⁻³. Using a ratiometric approach, C/H and H/O ratios showed a good correlation with the actual stoichiometric ratios and a partial identification success could be achieved. Finally employing principle component analysis, an excellent classification could be attained.

Keywords: Laser induced breakdown spectroscopy; Explosive detection; Principal component analysis; Multivariate analysis

NOMENCLATURE

- I Intensity
- k Boltzmann constant
- T plasma temperature
- h Plank`s constant
- I Partition function
- E_k Energy of the k^{th} energy level
- A_{ki} Transition probability from level k to i^{th} level
- g_k Degeneracy of the k^{th} energy level

1. INTRODUCTION

Laser induced breakdown spectroscopy (LIBS) is a laser based optical emission technique. It can provide valuable information about elemental constituents of a sample based on spectral content of the emitted light. Light from a pulsed laser source, of sufficient intensity, when focused onto the sample surface, results in instant thermalisation and evaporation of material and leads to the formation of plasma¹⁻³. A single laser pulse is sufficient to create a plasma which acts as a rich source of spectral emissions resulting in the LIBS spectrum, typically in the range of 200 nm - 900 nm. The plasma is characterised by temperature and electron density. The wavelength(s) of emitted light is characteristic of the atoms, ions, and molecular fragments present in the plasma, which represent the elemental constituents of the material under investigation. The assignment of the peaks can be accomplished by using the data available in NIST database⁴. Little sample preparation, nearly non-destructive, in-situ, multi-elemental detection, fast analysis and avoiding the wet chemistry combined with the ability

to probe matter in any of the three forms of matter even at remote/standoff distances makes LIBS a promising candidate for the futuristic applications. Any application(s), particularly those where the proximity to the sample is limited or restricted because of its hazardous nature, this technique can be one of the important tools in tool-box of analytical techniques. A variety of applications of this technique have been reported in diverse fields of pharmaceuticals⁵, nuclear⁶, biological⁷, explosives⁸, radiological⁹, archeological¹⁰, and planetary exploration¹¹.

In recent years, on account of increased threat to the homeland security, the efforts for detection of explosives and its related compounds has seen major thrust in the global community as well as India. LIBS can be a potential solution for application where the closer proximity of the operator to the sample is inaccessible/threatening or harsh environments. Standoff capability of LIBS offers a suitable choice for identification of hazardous materials including explosives in such situations, which otherwise is not possible by other conventional vapour based techniques like gas chromatography¹² and ion-mobility spectrometry (IMS)¹³⁻¹⁵. The standoff detection of explosives is a multifold challenging task where the signal strength decreases inversely with distance, inevitable losses in intensity arise due to atmospheric absorption/scattering of light and the possibility of the sample being present on varied types of materials. LIBS, as compared to other optical techniques like Raman, not only gives the abundant light signal but also the instrumentation is relatively simpler. Two distinct scenarios for detection of explosives can be envisaged - the former is the need to distinguish a material as explosive or non-explosive, such an application is relevant in airport baggage check. The latter being identification of the specific explosive, which

can give crucial inputs to the investigators to solve a bomb blast case. Stand-off/Remote applications of LIBS has been shown to give promising results in various fields like explosive detection⁸, nuclear waste management¹⁶, Mars exploration¹¹, Chandrayaan¹⁷, combustion¹⁸, and geology¹⁹. Laserna²⁰, *et al.* have shown the capability of LIBS at standoff distances of up to 120 m. The Mars rover's ChemCam instrument has LIBS sensor working at a distance of seven meters¹¹. Chandrayan II has a proposed onboard LIBS sensor. While signal strength and collection combined with several advantages make LIBS a contender for future, the applications related to the identification of explosives comes with an additional challenge. The spectra for a large class of samples, particularly the secondary explosives, which are primarily of the molecular form CHNO are strikingly similar. As LIBS is an elemental technique, the resulting spectra of these samples, and numerous other non-explosives materials like sugars, grease, oils, plastics, etc. will as well be primarily dominated by carbon, hydrogen, nitrogen and oxygen. The atmospheric oxygen/nitrogen and hydrogen from the humidity may further compound the problem. Though, visually the spectra may look similar and almost identical, but with the aid of suitable multivariate approaches, it is still possible to classify the samples. Wang²¹, *et al.* has shown discrimination among organic explosives and plastics using principal component analysis (PCA) and partial least squares-discriminant analysis (PLS-DA) on LIBS data. Sreedhar^{8,22}, *et al.* and De Lucia²³, *et al.* reported that intensity ratio could be utilised for identification of high energy materials (HEMs). Recognition of explosive residues in air using PCA was also attempted by Lazic²⁴, *et al.* Chemometrics multivariate analysis was employed to classify the pharmaceutical samples, explosives and isomers^{5,25-27} by our group. Lopez-Moreno²⁸, *et al.* demonstrated that peak ratio analysis combined with C₂ Swan band system could be used for identification of explosives. De Lucia²⁹, *et al.* has performed first time double pulse standoff LIBS technique for the detection of explosives and they demonstrated better discrimination for RDX residue and diesel fuel on Aluminum substrate compared to single pulse LIBS by reducing the atmospheric interference to plasma. Gottfried³⁰, *et al.* distinguished the explosive residues, bulk 1,3,5-Trinitroperhydro-1,3,5-triazine (RDX) and composition-B with the aid of double pulse method with the optimum interpulse separation time of 3 μ s. In this investigation, we have exploited PCA for the classification of a set of explosives and also employed bi-variate ratio approach to identify among a set of five explosives using data obtained from the samples located at a distance of 1m.

2. EXPERIMENTAL DETAILS

The details of the experimental setup used for recording the data can be found in literature^{5,8,31}, with the exception of the distance of the sample from the focussing lens. In brief, 532 nm laser pulses of 7 ns pulse duration from a Q-switched Nd: YAG were employed. The sample was kept at a distance of 100 cm from a plano-convex quartz lens of 100 cm focal length. The calculated theoretical spot size and irradiance was $\sim 100 \mu$ m and $\sim 33 \text{ GW/cm}^2$, respectively. The emitted light

was collimated by a lens (focal length 100 cm) and another lens (focal length 10 cm) focussed it into the optical fiber entrance. The other end of the fiber was fed to the spectrometer (Michelle ME5000, coupled with an iSTAR DH734 ICCD). The schematic diagram of experimental LIBS setup is shown in Fig. 1.

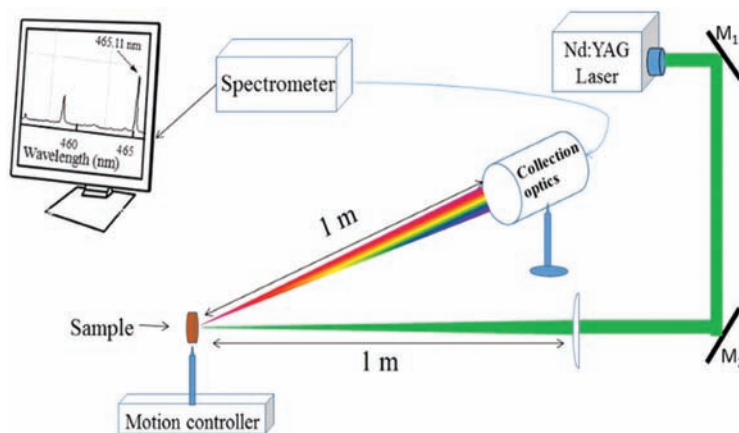


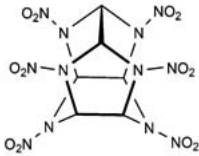
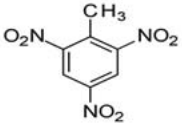
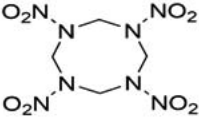
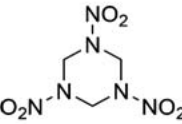
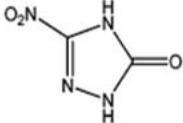
Figure 1. Schematic of LIBS Experimental setup.

Five explosive powders viz., 2,4,6,8,10,12-hexanitro-2,4,6,8,10,12-hexaazaisowurtzitane (CL20), Octahydro-1,3,5,7-tetranitro-1,3,5,7-tetrazocine (HMX), 5-Nitro-2,4-dihydro-3H-1,2,4-triazol-3-one (NTO), RDX, and 2,4,6-trinitrotoluen (TNT) were pressed into pellets and used to record the LIBS spectra. The details of the samples are given in Table 1. Laser pulses of 100 ± 2 mJ energy were focussed onto the sample surface for every laser exposure. Based on the availability of sample, a total 8-20 spectra were acquired for each explosive. The signal to noise ratio (SNR) was improved by the accumulation of five spectra. The SNR is evaluated by dividing the maximum value of a particular peak by the noise. The noise is defined as RMS of the signal on the baseline of the 40 adjacent pixels on either side of the evaluated peak³². The estimated SNR was 3.08 nm at 656.38 nm (Hydrogen peak) and is ~ 4 times lesser than the conventional LIBS setup where the plasma is produced and collected at a distance of 15 cm. All the spectra were recorded with a gate width of 10 μ s and a gate delay of 1 μ s.

3. RESULTS AND DISCUSSIONS

Typical LIBS spectra are illustrated in Fig. 2. Emission lines of carbon, hydrogen, nitrogen, oxygen, and calcium (labeled as C, H, N, O, and Ca at their corresponding strong lines on the spectra) were observed for all the samples. The spectra from all the explosives look similar, however, they differed in the intensities of the peaks. It can be noticed that carbon at 247.85 nm is the dominant peak followed by CN. The oxygen triplet, nitrogen, and hydrogen lines are observed at 777.42 nm, 746.89 nm, and 656.41 nm, respectively. Emissions from CN violet system and C₂ swan bands were observed at 384 nm - 389 nm, 516 nm, respectively. CN violet band (1,1), (2,2), (3,3), (4,4) transitions were seen at 387.10 nm, 386.13 nm, 385.42 nm, 385.01 nm, respectively. Table 2 shows relative intensities of the peaks and their corresponding emission wavelengths.

Table 1. First three columns represents the chemical formulae and chemical structure. The last six columns represents the various stoichiometric ratios.

Sample name	Chemical formulae	Chemical Structure	H/O	C/O	O/N	H/N	C/N	C/H
CL-20	C ₆ H ₆ N ₁₂ O ₁₂		0.5	0.5	1	0.5	0.5	1
TNT	C ₇ H ₅ N ₃ O ₆		0.83	1.17	2	1.67	2.33	1.4
HMX	C ₄ H ₈ N ₈ O ₈		1	0.5	1	1	0.5	0.5
RDX	C ₃ H ₆ N ₆ O ₆		1	0.5	1	1	0.5	0.5
NTO	C ₂ H ₂ N ₄ O ₃		0.67	0.67	.75	0.5	0.5	1

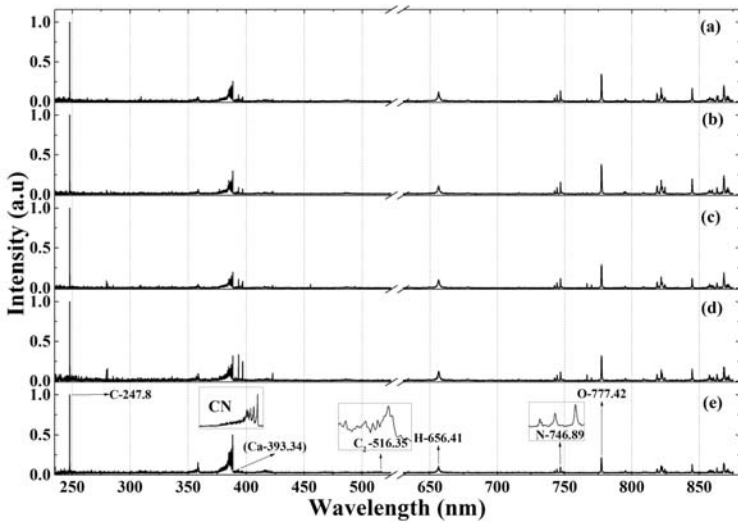


Figure 2 Typical LIBS spectra recorded for the samples (a) HMX, (b) CL-20, (c) NTO, (d) RDX and (e) TNT. All the spectra are normalised with respect to the Carbon peak at 247.85 nm.

3.1 Evaluation of Plasma Temperature and Electron Density

3.1.1 Measurement of Plasma Temperature

Temperature and electron density are the two important physical parameters of the plasma which influence the emission characteristics. The oxygen lines at 777.34 nm, 794.93 nm, and

844.65 nm have been used to estimate the temperature³³. The emission lines were fitted to a Lorentzian to obtain the height, area and width. The area under the curve is considered as the intensity (*I*) of the spectral line. The spectroscopic parameters were collected from NIST database⁴ and literature³³. The Intensity of a spectral line transition in the LIBS spectrum is given as

$$I = \frac{hcA_{ki}g_k}{4\pi\lambda P} N_0 \exp\left(\frac{-E_k}{K_B T}\right) \quad (1)$$

where N_0 is the total number of the atoms, k_B is Boltzmann constant, T is the temperature, h is planks constant, P is partition function, c is the speed of light. According to Boltzmann distribution, N_k the number of the atoms in the k^{th} energy level at a temperature T is given by -

$$N_k = \frac{N_0 g_k}{P} \exp\left(\frac{-E_k}{K_B T}\right) \quad (2)$$

By applying logarithm to Eqn 1, we get,

$$\ln\left(\frac{I\lambda}{A_{ki}g_k}\right) = -\frac{1}{k_B T} E_k + \ln\left(\frac{hcN_0}{4\pi P}\right) \quad (3)$$

By plotting E_k Vs $\ln\left(\frac{I\lambda}{A_{ki}g_k}\right)$ and fitting it to a straight line, the temperature was estimated, which is related to the slope of the line ($-1/kT$). Figure 3(a), shows a typical Boltzmann plot

Table 2. Relative Intensities of the spectral lines from TNT spectra.

Element	Wavelength (nm)	Normalised Intensity
Carbon	247.85	1.00
Hydrogen	656.41	0.10
Nitrogen	746.89	0.10
Oxygen	777.42	0.21
Sodium	589.00	0.05
Calcium	393.34	0.07
CN	388.29	0.49
C ₂	516.35	0.04

along with the straight line fit. The temperature estimated for all the samples are tabulated in Table 3. The error represents the standard deviation obtained from the multiple estimates obtained from different spectra. The evaluated temperatures are in the range of 9000 K - 12750 K and the average temperature over all the samples is 10900 K.

Table 3. Plasma temperature obtained from the oxygen lines of five explosives

Sample name	Plasma temperature (10 ³ K)
CL-20	10.4 ± 1.8
TNT	12.7 ± 3.2
HMX	11.1 ± 2.0
RDX	9.0 ± 1.8
NTO	11.3 ± 0.9

3.1.2 Measurement of Electron Density

The electron density of the plasma has been estimated from FWHM of the spectral line of O at 844.66 nm. The line is fitted to Lorentzian line shape using Matlab and a typical fit is shown in Fig. 3(b). As compared to Stark broadening (0.4 nm), Doppler (0.015 nm) and natural line width (0.0023 nm) are negligible and hence only Stark broadening is considered. The width of the emission line FWHM ($\Delta\lambda$) is related to electron density as

$$\Delta\lambda = 2\omega \left(\frac{N_e}{10^{16}} \right) \tag{4}$$

where ω is the impact width. Its value at 844.66 nm line is 0.05140 nm³⁴. As seen from Fig. 4(a), the electron density does not show significant difference across the samples. For all the samples the values are of the order of 10¹⁶ cm⁻³ and the mean for any sample is within the average standard deviation.

Under local thermodynamic equilibrium (LTE), the population and depopulation of the atoms in an excited state, are dominated by electron collisions rather than radiative process². The minimum electron density, a necessary but not sufficient condition required to follow LTE is given by McWhirter criterion³⁵ as –

$$N_e (\text{cm}^{-3}) \geq 1.6 \times 10^{12} T^{1/2} \Delta E^3 \tag{5}$$

where ΔE (eV) is the energy difference between spectral line transitions. The electron density obtained by Eqn. (5) is also shown Fig. 4(a) and it is evident that the plasma produced for all the samples satisfies the LTE condition.

As the peak intensity of the lines carry the information about the number density of the emitting species, it is vital to ascertain the optical thin condition. The branching ratio has been determined for all the samples to verify the optical thin condition. If the plasma doesn't satisfy the optical thin condition, then the self-absorption can affect the observed line intensities. The branching ratio is given as

$$\left(\frac{I_1}{I_2} \right) = \left(\frac{\lambda_{nm}}{\lambda_{ki}} \right) \left(\frac{A_{ki}}{A_{nm}} \right) \left(\frac{g_k}{g_n} \right) \exp \left(-\frac{E_k - E_n}{k_B T} \right) \tag{6}$$

where I_1 and I_2 are intensities of the two spectral lines originating from the same upper energy level. Oxygen lines at 777.42 nm and 844.4 nm were employed for the estimation of branching ratio and results are shown in Fig. 4(b)³³. It is clear from the figure that all the samples are satisfying the optical thin condition. The theoretical ratio is within in the standard deviation of the actual intensity ratio for all the samples. Considering that transition probabilities itself have 10 per cent uncertainty and hence observed branching ratios can be considered as a very good agreement³³.

The spectrum acquired from the optically thin plasma

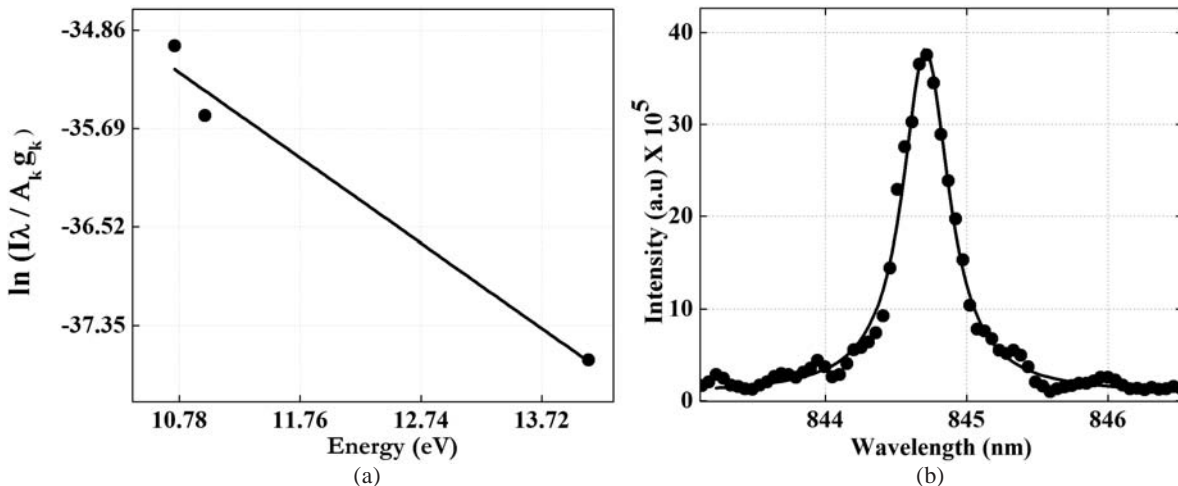


Figure 3. (a) The Boltzmann plot constructed, utilising the three oxygen lines of the CL-20 and (b) Lorentzian fit of oxygen spectral line at 844.67 nm of CL-20. The dots and continuous line represents the actual data and fitted data respectively.

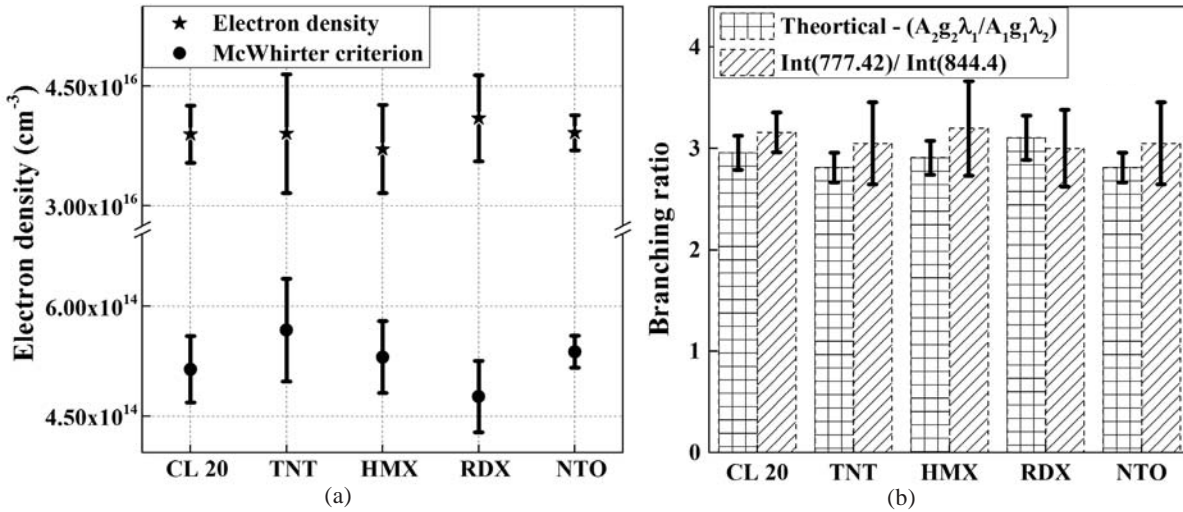


Figure 4. (a) The Electron density and McWhirter criterion obtained for the five samples for validating LTE condition and (b) Verifying the branching ratio condition by employing the intensity ratio of oxygen spectral lines.

which is under LTE, with the average temperature of 10910 K and electron density of $3.9 \times 10^{16} \text{ cm}^{-3}$, produced by focusing the laser light at 100 cm, will be utilised for the identification of the specific sample. First, different ratios and their correlation to the actual stoichiometry will be explored towards the identification of sample. As there is an overwhelming similarity among the spectra of all the explosives, the minute differences can be exploited by the judicious use of multivariate analysis. Multivariate analysis uses the intensity information available at all the 22290 wavelengths in the range of 220 nm - 850 nm.

3.2 Classification of Explosives from the Atomic Ratios

Ratios of different atomic lines viz., H/O, C/O, O/N, H/N, C/N and C/H from all the samples were considered to explore the correlation with the actual stoichiometry. As discussed in the last section, the area under the curve for an emission line is considered for the evaluation of ratios. The actual stoichiometric ratio implies the ratio of the number of atoms per molecule. For example, CL-20 (C₆H₆N₁₂O₁₂) has a C/N ratio of 0.5. Figure 5 shows the plot for O/N and C/O intensity ratios. The standard deviation obtained from multiple trails is depicted as an error bar. From the molecular formula of

RDX, HMX and CL20, it is evident that all the stoichiometric ratios are same except for H/O. Both the ratios do not provide any valuable information for the identification of the samples among themselves.

As seen from Fig. 5(a), the measured O/N ratio for all the samples have nearly same value of around 5.5 except for NTO. Only TNT can be clearly distinguished from all the samples with C/O as shown in Fig.5(b), it can also be observed that it has shown higher standard deviation among all the samples. Utilizing the C/N ratio (Figure not shown) a similar result was observed. CL20 and TNT have been shown clear apart from each other with the H/N (Figure not shown). It is also noticed that all the ratios of HMX and RDX are giving nearly identical values.

Figure 6 shows the plot for C/H and H/O. While C/H actual stoichiometry forms three sets of samples, it is not possible to distinguish among the samples with the same value for the ratio. However, an unknown sample can be identified as belonging to one of the three groups – a) RDX/HMX b) CL20/ NTO and c) TNT. With H/O, as shown in Fig. 6(b), the samples can be very well identified with the RDX and HMX forming a single group.

C/H ratio has a significant advantage over other ratios

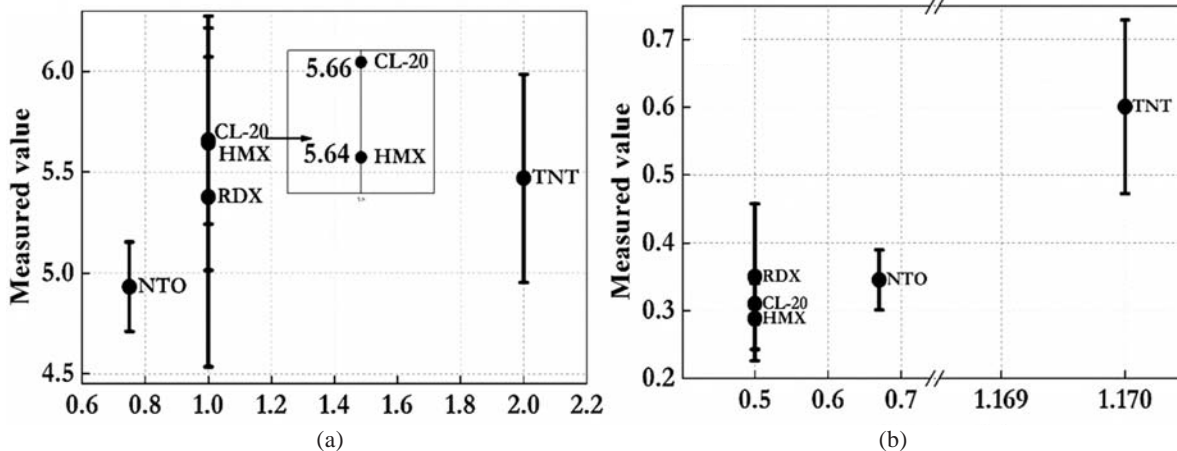


Figure 5. Comparison of the atomic ratios: (a) Actual value O/N and (b) Actual value C/O.

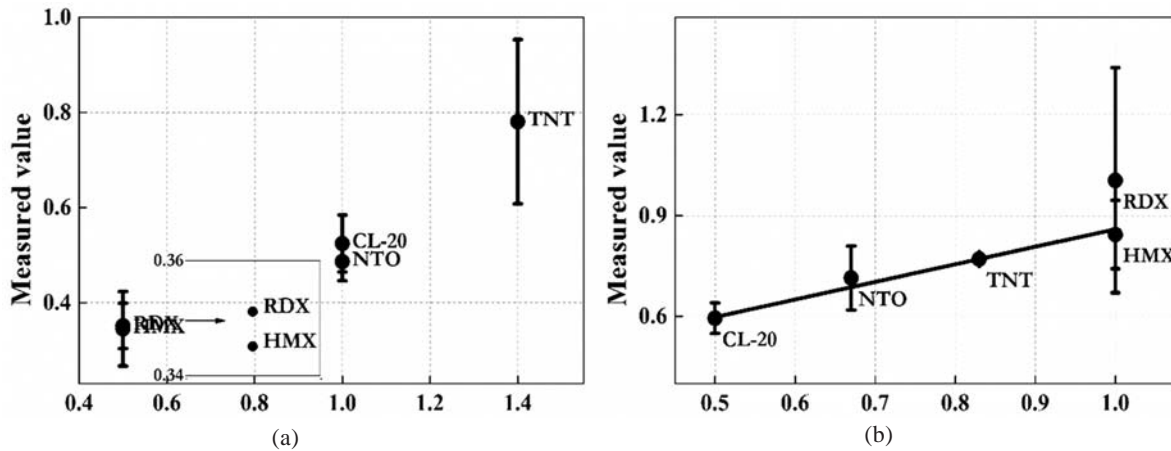


Figure 6. The comparison of the stoichiometric ratios with measured values (a) Atomic ratios of C/H and (b) H/O.

involving carbon or oxygen as it has a minimum effect of the atmospheric contribution to the plasma. Though C/H and H/O gives best results compared to other ratios, the performance is limited as none of them provide a clear distinction between all the samples studied.

3.3 Classification of Explosives by PCA

Typical spectra of all the five samples were overwhelmingly similar and application of ratios yielded a limited success in identification. In this section, multivariate analysis is employed to systematically investigate the presence of subtle differences between the spectra of each type of explosives. The advantage with the multivariate approach is that it considers the intensities at all the wavelengths rather than at some selected peaks. PCA is a technique that transforms the data into an 'abstract' space where the variables are the linear combinations of the original variables (different wavelengths).

Figure 7 shows the PCA cluster plot. Each data point, represented by co-efficients of first and the second principle components, represents a single LIBS spectrum in the transformed space. It can be seen that the spectra corresponding to an explosive sample now cluster together. As each spectrum is now represented by only two coordinates, PCA can also act as a data compression tool as well. The original spectra can be retrieved by multiplying the transformed data with the coefficient matrix, one of the outputs from the application of PCA. There are two outliers for TNT, three for NTO and one for RDX. The clear separation of the spectra in the principal component plane indicates that there are subtle but reproducible differences between the spectra of different explosives recorded from a distance of 1 m and enable their clear separation. The chemical basis of clustering, that is, the reason behind the clear separation of the clusters can be understood by looking at the individual principal components. The first and second PCs account for 75 per cent and 8 per cent of the variance respectively. The first five principal components, together account for 92.15 per cent of the net variance in the spectral dataset and 95 per cent is explained by first nine components. The first PC, which is the most dominant, contains the information from the carbon, hydrogen CN, oxygen, nitrogen and calcium. The second is mainly dominated by CN, C₂, oxygen, nitrogen

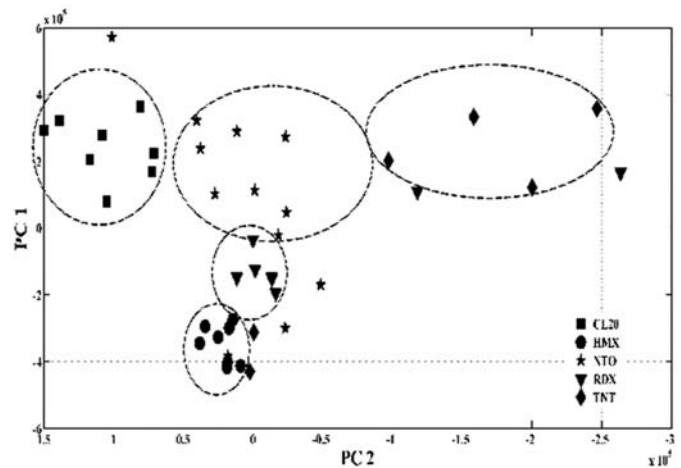


Figure 7. Score plot of first two principal components of explosive compounds.

calcium and sodium. Subsequent two PCs have combination of the elements in PC1 and PC2. The PCA data clearly establishes that the explosives studied in this article can be easily identified from the signal collected at a distance of 1 m.

The clustering is a clear indication that the spectra of different explosives have subtle but reproducible variations among themselves and can be harvested by applying suitable multivariate approach. Our group at ACRHEM is working to establish the standoff LIBS experiment in different configurations. The initial design consists of using a pair of convex-concave lenses for focusing at variable distances and a telescope for collection of signal, is underway. The work reported in this article is an initial experiment to demonstrate the identification of explosives based on the LIBS data recorded from a distance, where the signal to noise ratio reduces drastically compared to a collection from proximity. We are hopeful that with the establishment of above mentioned setup it will be possible for us to vary the standoff distances and also optimise the signal to noise ratio considerably with the reduced laser power.

4. CONCLUSIONS

LIBS signal of a set of secondary explosives has been recorded from a distance of 1 m. All the spectral signatures,

that can be seen using a close proximity system, could also be seen at the distance of 1 m. The plasma is characterised by estimating its temperature and electron density, which were in the range of $(10.9 \pm 2.1) \times 10^3$ K and electron density of $(3.9 \pm 0.5) \times 10^{16}$ cm⁻³, respectively. The plasma was optically thin as assessed by branching ratios satisfied McWhirter criterion which is necessary for the existence of LTE. From the ratiometric analysis, C/H and H/O are identified as best choice for ratios. These ratios could yield a partial classification of the explosive samples except for RDX and HMX. Both these samples have identical stoichiometric ratios and their average intensities fall within one standard deviation from each other. Finally, the potential of standoff LIBS for identification and classification of explosive compounds with PCA is demonstrated. An excellent separation is achieved where separate clusters for each explosive were observed in cluster plot. This indicates that the data recorded at a distance of 1 m has enough chemical information that can be utilised for identifying the explosives.

ACKNOWLEDGEMENTS

Authors acknowledge the financial support from Defence Research and Development Organisation (DRDO), India.

REFERENCES

1. Singh, J.P. & Thakur, S.N. Laser-induced breakdown spectroscopy. Elsevier, 2007.
2. Cremers, D.A. & Knight, A.K. Laser-Induced Breakdown Spectroscopy. Wiley Online Library, 2006.
3. Miziolek, A.W.; Palleschi, V. & Schechter, I. Laser induced breakdown spectroscopy. Cambridge University Press, 2006.
4. NIST Database, http://physics.nist.gov/PhysRefData/ASD/lines_form.html.
5. Myakalwar, A.K.; Sreedhar, S.; Barman, I.; Dingari, N. C.; Rao, S.V.; Kiran, P. P.; Tewari, S. P. & Kumar, G. M. Laser-induced breakdown spectroscopy-based investigation and classification of pharmaceutical tablets using multivariate chemometric analysis. *Talanta*, 2011, **87**, 53-59, doi: 10.1016/j.talanta.2011.09.040.
6. Sarkar, A.; Alamelu, D. & Aggarwal, S.K. Determination of trace constituents in thoria by laser induced breakdown spectrometry. *J. Nucl. Mater.*, 2009, **384**(2), 158-62, doi: 10.1016/j.jnucmat.2008.11.005.
7. Jaswal, B.B.S. & Singh, V.K. Analytical assessments of gallstones and urinary stones: A comprehensive review of the development from laser to LIBS. *Appl. Spectrosc. Rev.*, 2015, **50**(6), 473-98, doi: 10.1080/05704928.2015.1010206.
8. Sreedhar, S.; Gundawar, M.K. & Rao, S.V. Laser induced breakdown spectroscopy for classification of high energy materials using elemental intensity ratios. *Def. Sci. J.*, 2014, **64**(4), 332-38, doi: 10.14429/dsj.64.4741.
9. Cremers, D.A.; Beddingfield, A.; Smithwick, R.; Chinni, R.C.; Jones, C.R.; Beardsley, B. & Karch, L. Monitoring Uranium, Hydrogen, and Lithium and their isotopes using a compact laser-induced breakdown spectroscopy (LIBS) probe and high-resolution spectrometer. *Appl. Spectrosc.*, 2012, **66**(3), 250-61, doi: 10.1366/11-06314.
10. Giakoumaki, A.; Melessanaki, K. & Anglos, D. Laser-induced breakdown spectroscopy (LIBS) in archaeological science—applications and prospects. *Anal. Bioanal. Chem.*, 2007, **387**(3), 749-60, doi: 10.1007/s00216-006-0908-1.
11. Maurice, S.; Wiens, R.; Saccoccio, M.; Barraclough, B.; Gasnault, O.; Forni, O.; Mangold, N.; Baratoux, D.; Bender, S. & Berger, G. The ChemCam instrument suite on the Mars Science Laboratory (MSL) rover: Science objectives and mast unit description. *Space Sci. Rev.*, 2012, **170**(1-4), 95-166, doi: 10.1007/s11214-012-9912-2.
12. Grob, R.L. & Barry, E.F. Modern practice of gas chromatography. John Wiley & Sons, 2004.
13. Caygill, J. S.; Davis, F. & Higson, S. P. Current trends in explosive detection techniques. *Talanta*, 2012, **88**, 14-29, doi: 10.1016/j.talanta.2011.11.043.
14. Wallin, S.; Pettersson, A.; Östmark, H. & Hobro, A. Laser-based standoff detection of explosives: A critical review. *Anal. Bioanal. Chem.*, 2009, **395**(2), 259-74, doi: 10.1007/s00216-009-2844-3.
15. Lefferts, M. J. & Castell, M.R. Vapour sensing of explosive materials. *Anal. Methods*, 2015, **7**(21), 9005-17, doi: 10.1039/C5AY02262B.
16. Singh, M.; Karki, V.; Mishra, R.K.; Kumar, A.; Kaushik, C.; Mao, X.; Russo, R.E. & Sarkar, A. Analytical spectral dependent partial least squares regression: A study of nuclear waste glass from thorium based fuel using LIBS. *J. Anal. At. Spectrom.*, 2015, **30**(12), 2507-15, doi: 10.1039/c5ja00372e.
17. Laxmiprasad, A.; Sridhar Raja, V.; Goswami, A.; Rao, M.; Lohar, K. & Menon, S. Realization of empirical database and generation of calibration curves for precise quantitative analysis employing a mini-LIBS for Chandrayaan-2 rover. In 39th COSPAR Scientific Assembly, 2012.
18. Ctvrtnickova, T.; Mateo, M.P.; Yanez, A. & Nicolas, G. Application of LIBS and TMA for the determination of combustion predictive indices of coals and coal blends. *Appl. Surf. Sci.*, 2011, **257**(12), 5447-5451, doi: 10.1016/j.apsusc.2010.12.025.
19. Sallé, B.; Cremers, D.A.; Maurice, S.; Wiens, R.C. & Fichet, P. Evaluation of a compact spectrograph for in-situ and stand-off laser-induced breakdown spectroscopy analyses of geological samples on Mars missions. *Spectrochim. Acta, Part B*, 2005, **60**(6), 805-815, doi: 10.1016/j.sab.2005.05.007.
20. Laserna, J.; Reyes, R.F.; González, R.; Tobaría, L. & Lucena, P. Study on the effect of beam propagation through atmospheric turbulence on standoff nanosecond laser induced breakdown spectroscopy measurements. *Opt. Express*, 2009, **17**(12), 10265-276, doi: 10.1364/Oe.17.010265.
21. Wang, Q.-Q.; Liu, K.; Zhao, H.; Ge, C.-H. & Huang, Z.-W. Detection of explosives with laser-induced breakdown spectroscopy. *Frontiers of Physics*, 2012, **7**(6), 701-707, doi: 10.1007/s11467-012-0272-x.
22. Sreedhar, S.; Rao, S.V.; Kiran, P.P.; Tewari, S.P. & Kumar,

- G.M. Stoichiometric analysis of ammonium nitrate and ammonium perchlorate with nanosecond laser induced breakdown spectroscopy. *In SPIE Defense, Security, and Sensing*, 2010.
doi: 10.1117/12.850014.
23. De Lucia, F.C., Jr.; Harmon, R.S.; McNesby, K.L.; Winkel, R.J., Jr. & Miziolek, A.W. Laser-induced breakdown spectroscopy analysis of energetic materials. *Appl. Opt.*, 2003, **42**(30), 6148-6152.
doi: 10.1364/AO.42.006148.
 24. Lasic, V.; Palucci, A.; Jovicevic, S.; Poggi, C. & Buono, E. Analysis of explosive and other organic residues by laser induced breakdown spectroscopy. *Spectrochim. Acta, Part B*, 2009, **64**(10), 1028-39,
doi: 10.1016/j.sab.2009.07.035.
 25. Myakalwar, A. K.; Anubham, S.K.; Paidi, S.K.; Barman, I. & Gundawar, M.K. Real-time fingerprinting of structural isomers using laser induced breakdown spectroscopy. *Analyst*, 2016, **141**(10), 3077-83.
doi: 10.1039/C6AN00408C.
 26. Myakalwar, A. K.; Spegazzini, N.; Zhang, C.; Anubham, S.K.; Dasari, R.R.; Barman, I. & Gundawar, M.K. Less is more: Avoiding the LIBS dimensionality curse through judicious feature selection for explosive detection. *Sci. Rep.*, 2015, **5**, 13169.
doi: 10.1038/srep13169.
 27. Myakalwar, A.K.; Dingari, N. C.; Dasari, R.R.; Barman, I. & Gundawar, M.K. Non-gated laser induced breakdown spectroscopy provides a powerful segmentation tool on concomitant treatment of characteristic and continuum emission. *PLoS one*, 2014, **9**(8), e103546.
doi: 10.1371/journal.pone.0103546.
 28. Lopez-Moreno, C.; Palanco, S.; Laserna, J. J.; DeLucia Jr, F.; Miziolek, A. W.; Rose, J.; Walters, R. A. & Whitehouse, A.I. Test of a stand-off laser-induced breakdown spectroscopy sensor for the detection of explosive residues on solid surfaces. *J. Anal. At. Spectrom.*, 2006, **21**(1), 55-60.
doi: 10.1039/B508055J.
 29. De Lucia, F.C.; Gottfried, J.L.; Munson, C.A. & Miziolek, A.W. Double pulse laser-induced breakdown spectroscopy of explosives: Initial study towards improved discrimination. *Spectrochim. Acta, Part B*, 2007, **62**(12), 1399-04.
doi: 10.1016/j.sab.2007.10.036.
 30. Gottfried, J. L.; De Lucia, F. C.; Munson, C. A. & Miziolek, A. W. Double-pulse standoff laser-induced breakdown spectroscopy for versatile hazardous materials detection. *Spectrochim. Acta, Part B*, 2007, **62**(12), 1405-11.
doi: 10.1016/j.sab.2007.10.039.
 31. Dingari, N.C.; Barman, I.; Myakalwar, A. K.; Tewari, S. P. & Kumar Gundawar, M. Incorporation of support vector machines in the LIBS toolbox for sensitive and robust classification amidst unexpected sample and system variability. *Anal Chem*, 2012, **84**(6), 2686-94,
doi: 10.1021/ac202755e.
 32. Fisher, B.T.; Johnsen, H.A.; Buckley, S.G. & Hahn, D. W. Temporal gating for the optimization of laser-induced breakdown spectroscopy detection and analysis of toxic metals. *Appl. Spectrosc.*, 2001, **55**(10), 1312-19.
doi: 10.1366/0003702011953667.
 33. Hegazy, H. Oxygen spectral lines for diagnostics of atmospheric laser-induced plasmas. *Appl. Phys. B*, 2010, **98**(2-3), 601-606.
doi: 10.1007/s00340-009-3670-1.
 34. Griem, H. Spectral line broadening by plasmas. Academic Press, New York, 1974.
 35. McWhirter, R. Spectral intensities. 1965.

CONTRIBUTORS

Mr Rajendhar Junjuri received his BSc from Kakatiya University, Warangal, in 2009 and MSc from Osmania University, Hyderabad. Currently pursuing his PhD from Advanced Centre of Research in High Energy Material, University of Hyderabad. His is currently working in the field of laser spectroscopy. The main activities includes the identification and classification of materials through Laser induced breakdown Spectroscopy (LIBS) /Raman/IR with the main focus on high energy materials, isomers and polymers. He was involved in fine tuning of results, writing and correcting the manuscript and organising the references.

Dr Ashwin kumar Myakalwar has obtained his PhD (physics) from University of Hyderabad, in 2016. Currently working as a postdoctoral researcher at Institute of photonics and electronics, Prague, Czech Republic. His principal research interests are lie in the field of laser matter interaction, plasma spectroscopy, laser instrumentation, nonlinear optics, multivariate analysis, laser based methods and spectroscopy (such as LIBS, Raman, Fluorescence and IR absorption spectroscopy). He has assisted in performing the experiment and writing the manuscript.

Dr Manoj Kumar Gundawar obtained his PhD from University of Hyderabad, in 2005. Presently working as Assistant Professor at Advanced Centre of Research in High Energy Materials, University of Hyderabad. His primary research interest is spectroscopy (LIBS and Raman spectroscopy), light-matter interactions and smart instrument design based on treatment of spectroscopic data using multivariate chemometrics analysis. He has conceived the idea presented in this paper, planned the work, and assisted in data analysis and writing the manuscript.